Influence of flow constraints on the properties of the critical endpoint of symmetric nuclear matter

A. I. Ivanytskyi,[1,2] K. A. Bugaev,[1] V. V. Sagun,[1,3] L. V. Bravina,[4] and E. E. Zabrodin[4,5,6]

[1]*Bogolyubov Institute for Theoretical Physics of the National Academy of Sciences of Ukraine, Metrologichna str. 14b, 03680 Kiev, Ukraine*
[2]*Department of Fundamental Physics, University of Salamanca, Plaza de la Merced s/n 37008, Spain*
[3]*Centro Multidisciplinar de Astrofísica, Instituto Superior Tecnico, Universidade de Lisboa, Av. Rovisco Pais 1, 1049-001 Lisboa, Portugal*
[4]*Department of Physics, University of Oslo, Sem Sælands vei 24, 0371 Oslo, Norway*
[5]*National Research Nuclear University (MEPhI), Kashira Highway 31, 115409 Moscow, Russia*
[6]*Skobeltsyn Institute of Nuclear Physics, Lomonosov Moscow State University, Leninskie gory, GSP-1, 119991 Moscow, Russia*

We propose a novel family of equations of state for symmetric nuclear matter based on the induced surface tension concept for the hard-core repulsion. It is shown that having only four adjustable parameters the suggested equations of state can, simultaneously, reproduce not only the main properties of the nuclear matter ground state, but the proton flow constraint up its maximal particle number densities. Varying the model parameters we carefully examine the range of values of incompressibility constant of normal nuclear matter and its critical temperature, which are consistent with the proton flow constraint. This analysis allows us to show that the physically most justified value of nuclear matter critical temperature is 15.5–18 MeV, the incompressibility constant is 270–315 MeV and the hard-core radius of nucleons is less than 0.4 fm.

I. INTRODUCTION

The determination of basic characteristics of symmetric nuclear matter and possible interrelations between them is of fundamental importance [1–6] not only for nuclear spectroscopy and for nuclear physics of intermediate energies, but also for nuclear astrophysics in view of possible phase transformations in compact astrophysical objects (neutron stars, hypothetical hybrid, and quark stars). From the practical point of view such characteristics of infinite nuclear matter as the normal density n_0 at zero pressure and zero temperature, its binding energy per nucleon W_0, and its incompressibility factor K_0 are of great importance for various phenomenological models because just these characteristics are used to fix the model parameters. Furthermore, such parameters of the nuclear liquid-gas transition phase diagram as the critical temperature T_c, the critical particle number density n_c, and critical pressure p_c at the endpoint and the values of critical exponents are important not only for the theory of critical phenomena, but they are also important for a verification of the novel theoretical approaches to study the phase transitions in finite systems with strong interaction [5,7–11].

Although some of these parameters, namely n_0 and W_0 are known well, the model-independent experimental determination of all other aforementioned characteristics is extremely difficult, since these parameters correspond to an infinite nuclear matter, while in the experiments one can study only the nuclei of finite size. Therefore, any relations or conditions that connect these characteristics are very important both for nuclear theory and for experiment. Recently, a comprehensive analysis of the relation between the critical temperature of hot nuclear matter and incompressibility factor of its ground state, i.e., at the particle number density n_0 and vanishing temperature, was performed in Refs. [12,13] for relativistic

mean-field (RMF) models. One of the important constraints imposed on the RMF models discussed in Refs. [5,12] is the so-called proton flow constraint [14]. This constraint [14] requires that at vanishing temperature and high baryonic charge densities the realistic equations of state (EoS) are soft, i.e., it sets rather strong restrictions on the particle number density dependence of pressure from two to about five values of normal nuclear density. As a result, even having about ten or more adjustable parameters, only 104 RMF models out of 263 analyzed in Ref. [5] are able to obey this constraint. It is clear that so many model parameters do not allow us to perform a systematic study of the flow constraint influence on the characteristics of symmetric nuclear matter critical endpoint (CEP) for the RMF models.

At the same time, two novel approaches to account for the hard-core repulsion in relativistic quantum gases were suggested recently [15,16]. Their advantage is that the novel EoSs allow one to go beyond the usual van der Waals approximation [15,16]. However, the EoS developed in Ref. [15] employs the parametrizations of attractive interaction, which are typical for classical gases and, as a result, even the minimal value obtained for the incompressibility factor K_0 is somewhat above its experimental range of nuclear matter [5,12,13,17], while the values of nucleon hard-core radius are too large. Furthermore, in Ref. [16] it is shown that for the same parametrization of the mean-field attractive potential and temperatures below 1 MeV the EoS that belong to the class suggested in Ref. [16] are essentially softer than their analogs developed in Ref. [15]. Therefore, in order to study the influence of the proton flow constraint it is natural to use a softer EoS from the class suggested in Ref. [16]. For this purpose here we formulate a family of four-parametric EoSs with the phenomenological attraction similar to that in

Ref. [18], which are normalized to the properties of nuclear matter ground state and satisfy the proton flow constraint. Using this EoS family, we perform a systematic investigation of restrictions on the critical temperature T_c and incompressibility factor K_0 generated by the flow constraint [14]. This study allows us to show that the critical compressibility factor Z_c of nuclear matter can be essentially lower than the typical values 0.28–0.31 obtained by the RMF models [13] and, hence, it can be similar to the Z_c values of ordinary nonorganic liquids. Based on these results, we believe that the present approach enables us to make a bridge between the nuclear matter EoS and the ones for ordinary liquids.

The work is organized as follows. The main ingredients of a novel EoS are given in Sec. II. Section III is devoted to a systematic analysis of the proton flow constraint influence on the nuclear matter EoS and its CEP properties. Our conclusions are given in Sec. IV.

II. EQUATION OF STATE

Since we develop a phenomenological model of nuclear matter, we are not bound by the Lagrangian choice and, hence, we consider only the nucleons assuming that effect of the Δ and heavier baryonic resonances, which can appear at high densities is absorbed in the mean fields. The hard-core repulsion in the present model is treated within a framework of the induced surface tension Σ developed in Ref. [9]. The model pressure p and Σ are a solution of the system (R is the hard-core radius on nucleons)

$$p = p_{id}(T, \nu_p) - p_{\text{int}}[n_{id}(T, \nu_p)], \quad (1)$$

$$\Sigma = R \, p_{id}(T, \nu_\Sigma), \quad (2)$$

where $p_{id}(T, \mu)$ is the grand canonical pressure of noninteracting pointlike fermions

$$p_{id}(T, \nu) = T g \int \frac{d^3 p}{(2\pi)^3} \ln \left[1 + \exp \left(\frac{\nu - \sqrt{p^2 + m^2}}{T} \right) \right], \quad (3)$$

and the particle number density is defined as

$$n_{id}(T, \nu) = \frac{\partial p_{id}}{\partial \nu} = g \int \frac{d^3 p}{(2\pi)^3} \frac{1}{\exp \left(\frac{\sqrt{p^2 + m^2} - \nu}{T} \right) + 1}. \quad (4)$$

Here the system temperature is T, $m = 940 \, \text{MeV}$ is the nucleon mass and the nucleon degeneracy factor is $g = 4$.

The term $-p_{\text{int}}$ in Eq. (1) represents the mean-field contribution to the pressure caused by an attraction between the nucleons. Of course, the repulsive scattering channels are also present in nuclear matter. However, at densities below $n_{\text{max}} \simeq 0.75 \, \text{fm}^{-3}$, which is the maximal density of the flow constraint [14], they are suppressed by the presence of attractive ones. Indeed, for such value of particle number density the average nucleon separation is about $r_{\text{min}} = \left(\frac{3}{4\pi n_{\text{max}}} \right)^{1/3} \simeq 0.7 \, \text{fm}$. At such a separation the microscopic nucleon-nucleon potential is attractive [19–21], while the residual repulsive interaction can be safely accounted for by the particle hard-core repulsion.

The quantity Σ in Eq. (2) is the surface tension induced by the hard-core repulsion between the nucleons and, hence, in Ref. [9] it was called the induced surface tension (IST)

in order to distinguish it from the eigensurface tension of ordinary nuclei. Appearance of the IST is caused by the fact that virial expansion of the pressure includes the terms that are proportional not only to the eigenvolume $V_0 = \frac{4\pi}{3} R^3$, but also to the eigensurface $S_0 = 4\pi R^2$ of a particle with the hard-core radius R. The surface term contribution is accounted for by the induced surface tension coefficient Σ. The meaning of this quantity as the surface tension coefficient can be easily seen from the effective chemical potentials, which are defined through the baryonic chemical potential μ as

$$\nu_p = \mu - p V_0 - \Sigma S_0 + U[n_{id}(T, \nu_p)], \quad (5)$$

$$\nu_\Sigma = \mu - p V_0 - \alpha \Sigma S_0 + U_0, \quad (6)$$

where Σ, indeed, is conjugated to S_0 and the attractive mean-field potentials are $U[n_{id}(T, \nu_p)]$ and $U_0 = \text{const}$. From these equations we conclude that the effects of hard-core repulsion are only partly accounted for by the eigenvolume of particles, while the rest comes through their eigensurface and, consequently, through the IST coefficient (for a detailed discussion see Ref. [9]). It is also worth to note that the presence of the ideal gas pressures p_{id} in Eqs. (1)–(2) is typical for EoSs, which are formulated in the grand canonical ensemble formalism. For example, the well known van der Waals EoS without attraction can be written as $p_{VdW} = p_{id}(T, \mu - 4p V_0)$ [22].

The system (1)–(6) is a concrete realization of the quantum model suggested in Ref. [16], where the self-consistency condition

$$p_{\text{int}}(n) = n \, U(n) - \int_0^n dn' \, U(n'), \quad (7)$$

was thoroughly discussed for the EoS of the same class as the one defined by Eqs. (1)–(6). Equation (7) relates the interaction pressure $p_{\text{int}}[n_{id}(T, \nu_p)]$ and the corresponding mean-field potential $U[n_{id}(T, \nu_p)]$ and it guarantees the fulfillment of all thermodynamic identities [16].

Note that by substituting the constant potential $U_0[n_{id}(T, \nu_\Sigma)] = \text{const}$ into the consistency condition (7) one automatically obtains that the corresponding mean-field pressure should be zero, i.e., $\tilde{p}_{\text{int}}[n_{id}(T, \nu_\Sigma)] = 0$. Different density dependence of the attractive mean-field potentials $U(n_{id})$ and U_0 reflects the different origins of their forces, namely $U[n_{id}]$ is generated by the bulk part of interaction, while U_0 is attributed to the surface part. The meaning of U_0 potential can be understood after the nonrelativistic expansion of the particle energy $\sqrt{m^2 + k^2} \simeq m + \frac{k^2}{2m}$ in the momentum distribution function in Eq. (4): U_0 decreases the nucleon mass to the value $m - U_0$, which resembles the RMF approach.

Finding the partial μ derivatives of Eqs. (1) and (2), one can get the particle number density from the usual thermodynamic identity

$$n = \frac{\partial p}{\partial \mu} = \frac{n_{id}(T, \nu_p)}{1 + V_0 n_{id}(T, \nu_p) + \frac{3 V_0 n_{id}(T, \nu_\Sigma)}{1 + 3(\alpha - 1) V_0 n_{id}(T, \nu_\Sigma)}}. \quad (8)$$

In principle, Eq. (2) for the IST coefficient could contain the interaction pressure $\tilde{p}_{\text{int}}(n_{id}(T, \nu_\Sigma)$ [16]. However, since the

pioneering work [22], in which the van der Waals-like hard-core repulsion, i.e., the term $-pV_0$ in Eq. (5), was introduced into the RMF model of nuclear matter, it is well known that such a repulsion is very weak at the vicinity of the nuclear matter ground state because in this region $p \simeq 0$ and, hence, an additional repulsion is absolutely necessary. In Ref. [22] the additional repulsion was provided by a vector meson field interacting with nucleons, while here such a repulsion is exclusively provided by the IST coefficient Σ. Hence, its interaction pressure $\tilde{p}_{\text{int}}[n_{id}(T, \nu_\Sigma)]$ could not contain any attraction in contrast to the term $p_{\text{int}}[n_{id}(T, \nu_p)]$ in Eq. (1). As it was shown in Refs. [23–25] exactly the form of Eq. (2), i.e., with $\tilde{p}_{\text{int}}[n_{id}(T, \nu_\Sigma)] \equiv 0$, allows one to correctly account for the hard-core repulsion in case of the Boltzmann statistics up to the packing fractions $\eta \equiv V_0 n \simeq 0.2$ (here n is the particle number density), if the parameter α is chosen as $\alpha = 1.245$. An additional reason for such a simple parametrization of Eq. (2) is to keep the number of parameters as small as possible. Due to the same reason for the present model we fix $\alpha = 1.245$.

The role of the parameter $\alpha = 1.245$ can be seen from the expression for the particle number density (8). Indeed, from Eq. (8) one can see that at low pressures, when the excluded volume effects are weak and the system is close to the nonrelativistic ideal gas, i.e., for $\nu_p \ll m$, $\nu_\Sigma \ll m$ and the temperatures $|\nu_p - \nu_\Sigma| \ll T \ll m$, then the densities $n_{id}(T, \nu_p)$ and $n_{id}(T, \nu_\Sigma)$ are simply equal to each other, i.e., $n_{id}(T, \nu_p) \simeq n_{id}(T, \nu_\Sigma)$, and, hence, the particle number density $n \simeq \frac{n_{id}(T, \nu_p)}{1 + 4 V_0 n_{id}(T, \nu_p)}$ acquires the typical one component excluded volume (EV) form [26]. The last equality was obtained from Eq. (8) under an evident approximation that at low pressures and densities the term $V_0 n_{id}(T, \nu_\Sigma) \ll 1$ is small and can be neglected. Thus, at low pressures the system (1)–(6) recovers the usual excluded volume results by construction.

At higher pressures the situation is defined by the value of parameter α. If $\alpha < 1$, then at some value of $n_{id}(T, \nu_\Sigma) = \frac{1}{3(1-\alpha)V_0} > 0$ the particle number density vanishes and further increase of pressure makes it negative. Hence, we conclude that the case $\alpha < 1$ is unphysical. If $\alpha > 1$, then at high pressures both densities $n_{id}(T, \nu_p)$ and $n_{id}(T, \nu_\Sigma)$ diverge and the particle number density becomes equal to the inverse value of nucleon eigenvolume $n \to 1/V_0$. This feature of the present EoS is caused by an accurate parametrization of the hard-core repulsion effects for $\alpha > 1$. Therefore, by fixing $\alpha = 1.245$ we keep the connection to the results obtained for the Boltzmann statistics at high temperatures [23–25].

If, however, in a special case $\alpha = 1$, then at high pressures the behavior of particle number density $n = \frac{n_{id}(T, \nu_p)}{1 + V_0 n_{id}(T, \nu_p) + 3 V_0 n_{id}(T, \nu_\Sigma)}$ strongly depends on the details of the model interaction. Thus, for $\mu \to \infty$ one finds that $\nu_p - \nu_\Sigma = U[n_{id}(T, \nu_p)] - U_0$. If the function $U[n_{id}(T, \nu_p)]$ corresponds to an attraction and it is a growing function of its argument $n_{id}(T, \nu_p)$, then in this limit one finds $n_{id}(T, \nu_p) \gg n_{id}(T, \nu_\Sigma)$ and, therefore, $n \to 1/V_0$. Apparently, the speed of approaching the limiting value depends on the strength of mean-field potentials $U(n)$ and U_0. Now it is clear that for the case of repulsion, i.e., for $U[n_{id}(T, \nu_p)] < 0$, the particle number density $n \to \frac{n_{id}(T, \nu_p)}{3 V_0 n_{id}(T, \nu_\Sigma)} \ll 1/V_0$. It can be even lower than for the classical excluded volume approximation. This is, actually,

one of the reasons of why the repulsion of the present model is exclusively described by the hard-core repulsion, which allows one to avoid such problems for $\alpha > 1$.

III. NUCLEAR MATTER PROPERTIES

In this work we use the power parametrization of the mean-field potential motivated by Ref. [18]. i.e.,

$$U(n) = C_d^2 n^\kappa \quad \Rightarrow \quad p_{\text{int}}(n) = \frac{\kappa}{\kappa + 1} C_d^2 n^{\kappa+1}, \qquad (9)$$

where the mean-field contribution to the pressure $p_{\text{int}}(n)$ is obtained from the consistency condition (7). Note that this is one of the simplest choices of the mean-field potential, which includes two parameters only, i.e., C_d^2 and κ. Since the parameter α is fixed the other two parameters of the IST model are the hard-core radius R and the constant potential U_0. Also it is important that in a general way one can show that in contrast to other phenomenological EoS the present one obeys the third law of thermodynamics [16]. Furthermore, recently EoS of this type was successfully applied for modeling the neutron star interiors [27]. We consider this as another argument in favor of simple parametrization given by Eq. (9).

The IST EoS with four adjustable parameters allows one to simultaneously reproduce the ground-state properties of symmetric nuclear matter, i.e., it has a vanishing pressure $p = 0$ at zero temperature and the normal nuclear particle number density $n_0 = 0.16$ fm^{-3} and the value of its binding energy per nucleon $W_0 = \frac{\epsilon}{n} - m = -16$ MeV (here ϵ denotes the energy density) and, hence, the corresponding chemical potential is $\mu = 923$ MeV. The present EoS with the attraction term (9) was normalized to these properties of nuclear matter ground state and, simultaneously, it was fitted to obey the proton flow constraint. It is necessary to stress that effects of the symmetry energy were systematically studied and found to be insignificant for description of the proton flow data [14]. Furthermore, in Ref. [28] the same conclusion was drawn based on the thorough analysis of a rich collection of the nuclear matter EoSs, which are able to reproduce the maximal value of mass of observed neutrons stars. Thus, the flow constraint is sensitive only to the isospin independent part of the nuclear matter EoS and, consequently, it can be safely studied with the symmetric nuclear matter EoS. In our analysis we considered several values of parameter $\kappa = 0.1, 0.15, 0.2, 0.25$, and 0.3. For a fixed value of parameter κ the two curves in the n-p plane were found in such a way that the upper curve is located not above the upper branch of the flow constraint, while the lower one is located not below the lower branch of this constraint. The details are clear from Figs. 1 and 2. These are highly nontrivial results for an EoS with only four adjustable parameters, since to parametrize the proton flow constraint alone one needs at least eight independent points. One can readily check that all parametrizations of the IST EoS shown in Figs. 1 and 2 also obey the kaon production constraint obtained in Ref. [29] for the symmetric nuclear matter pressure in the following range $1.2 \, n_0 < n < 2.2 \, n_0$ of the particle number density n.

The larger values of parameter κ were not considered, since the good description of the proton flow constraint cannot be achieved for $\kappa \geqslant 0.33$. The reason is apparent from the bottom
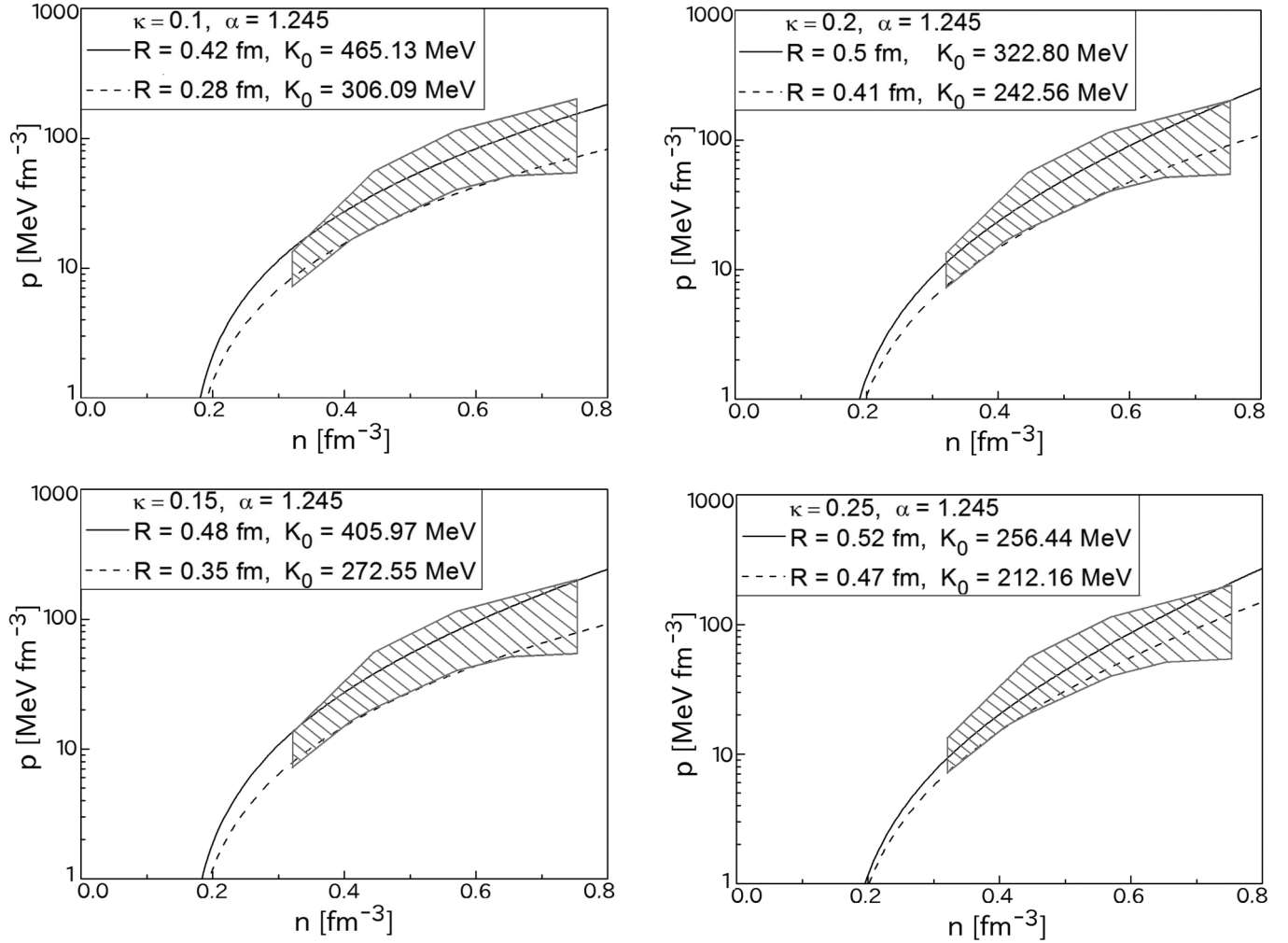
FIG. 1. Density dependence of the system pressure is shown for several sets of parameters, which are specified in the legend of each panel. See Table I for more details. The dashed area corresponds to the proton flow constraint of Ref. [14].

FIG. 2. Same as in Fig. 1, but for $\kappa = 0.2, 0.25,$ and 0.3.

panel of Fig. 2. The values of parameter κ below 0.1 were not considered as well because they correspond to very large values of the incompressibility constant $K_0 \equiv 9 \frac{\partial p}{\partial n}|_{T=0,n=n_0}$. As one can see from Table I for $\kappa = 0.1$ the minimal value of the incompressibility constant K_0 is about 306 MeV, while for $\kappa < 0.1$ it gets even larger.

Of course, we employed the other parametrizations of the attractive mean-field potential $U(n)$ as well, namely the van der Waals one $U(n) = 2an - 4V_0 an^2$, the constant one $U(n) = c$, and the Clausius one $U(n) = \frac{a}{c}(1 - \frac{1}{(1+cn)^2})$ with the constant values of parameters a and c, but none of them gave as good results, as we found for the parametrization (9) with $\alpha = 1.245$. Therefore, we believe that the IST EoS with the attraction (9) catches the correct physics from the normal nuclear density up to the maximal particle number density $n_{\max} \simeq 0.75$ fm^{-3} of the proton flow constraint.

Similarly to all models with the mean-field attraction the IST EoS has the liquid-gas phase transition, whose line ends at the CEP. The latter is defined as an inflection point in the
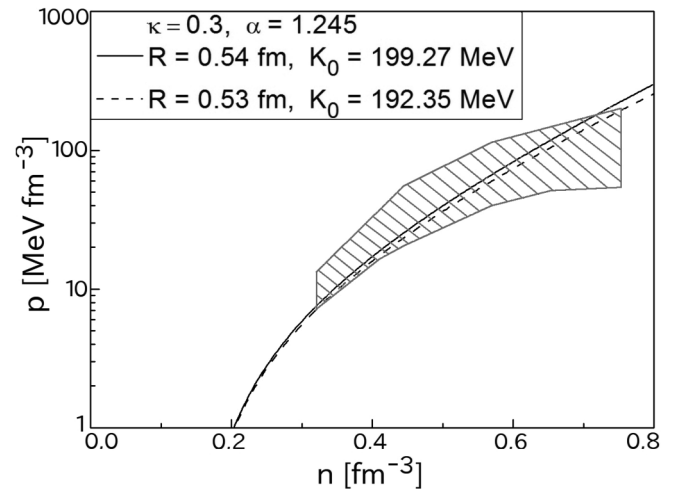
n-p plane. In other words, at CEP one finds

$$\frac{\partial p}{\partial n} = 0, \quad \frac{\partial^2 p}{\partial n^2} = 0. \tag{10}$$

TABLE I. Different sets of parameters which simultaneously reproduce the properties of normal nuclear matter ($p = 0$ and $n = n_0 = 0.16$ fm^{-3} at $\mu = 923$ MeV, see text for details) and obey the proton flow constraint on the nuclear matter EoS along with incompressibility factor K_0 and parameters of CEP. $R, C_d^2, U_0,$ and κ are the adjustable parameters of EoS, while the baryonic chemical potential μ_c, T_c, particle number density n_c, pressure p_c and compressibility constant $Z_c \equiv \frac{p_c}{T_c n_c}$ at CEP are found for each set of model parameters.

	$\kappa = 0.1$		$\kappa = 0.15$		$\kappa = 0.2$		$\kappa = 0.25$		$\kappa = 0.3$	
R(fm)	0.28	0.42	0.35	0.48	0.41	0.50	0.47	0.52	0.53	0.54
C_d^2(MeV fm$^{3\kappa}$)	284.98	325.06	206.05	229.57	168.15	179.67	146.97	152.00	133.79	134.60
U_0(MeV)	567.32	501.65	343.93	312.83	231.42	217.76	162.03	157.41	114.32	113.84
K_0(MeV)	306.09	465.13	272.55	405.97	242.56	322.80	217.16	256.44	192.35	199.27
μ_c(MeV)	890.94	881.01	900.08	895.08	906.44	904.49	911.11	910.53	914.74	914.70
T_c(MeV)	17.62	20.60	15.60	17.97	13.93	15.36	12.49	13.20	11.16	11.30
n_c(fm^{-3})	0.009	0.010	0.013	0.014	0.016	0.017	0.018	0.020	0.022	0.022
p_c(MeV fm^{-3})	0.0186	0.028	0.031	0.045	0.043	0.055	0.053	0.061	0.060	0.062
Z_c	0.1173	0.1359	0.1529	0.1789	0.1929	0.2106	0.2357	0.2311	0.2444	0.2494

The IST EoS supplemented by these conditions allows us to define critical temperature T_c, chemical potential μ_c, density n_c, and pressure p_c of the present model. The obtained results are summarized in Fig. 3 and in Table I. In Fig. 3 we divided the range of K_0 values into two regions, namely the lower one $K_0 = [200, 250]$ MeV and the upper one $K_0 = [250, 315]$ MeV. The lower region of K_0 values corresponds to the traditional experimental estimates (see a discussion in Ref. [5]), while the upper one corresponds to the more recent estimates given in Ref. [17]. The proton flow constraint defines the allowed region of K_0 and critical temperature T_c values, which are located between the lines ABC and FED in Fig. 3. From Fig. 3 one can see that the lower region of K_0 values determines the rectangle ABEF for the corresponding T_c values, while the upper one determines the rectangle BCDE. The obtained range of values is very similar to the results of

RMF models and the nonrelativistic mean-field ones discussed in Ref. [12].

However, the IST EoS allows one to obtain an essentially narrower range of K_0 and T_c values. Indeed, if one requires that this EoS should be applicable at the maximal value of particle number density $n_{\max} \simeq 0.75$ fm^{-3} of the proton flow constraint, then such a condition acquires the form

$$\tfrac{4}{3}\pi R^3 n_{\max} \leqslant \eta_{\max}, \tag{11}$$

where the range of the model applicability is given by the maximal packing fraction $\eta_{\max}$ of the model. Assuming that the maximal packing fraction of the present model is $\eta_{\max} = 0.2$, i.e., it is similar to the Boltzmann version of the IST EoS [23–25], one finds the following restriction on the nucleon hard-core radius $R \leqslant 0.4$ fm. This border line is shown in Fig. 3 by the short dashed line BG. It is necessary to stress that the value 0.4 fm is only 10% larger than the hard-core radius of baryons recently determined within the IST formulation of the hadron resonance gas model from fitting the hadronic multiplicities measured in central nuclear collisions at the AGS, SPS, RHIC, and LHC energies [23–25].

If, however, the present model has a wider range of applicability, i.e., $\eta_{\max} = 0.3$, then the inequality for the nucleon hard-core radius becomes $R \leqslant 0.45$ fm. It is shown in Fig. 3 by the long dashed line JH. Since there is no reason to expect that the quantum version of the IST EoS is applicable at the packing fractions exceeding the value $\eta_{\max} = 0.3$ we consider it as an upper limit of the model applicability. Alternatively, this means that the value 0.45 fm is an upper limit for the hard-core radius of nucleons.

The weak radius constraint $R \leqslant 0.45$ fm immediately reduces the range of K_0 and T_c values to the triangle JCH in Fig. 3. The strong radius constraint $R \leqslant 0.4$ fm defines even smaller triangle BCG of the allowed K_0 and T_c values in Fig. 3. Note that for the constraint $R \leqslant 0.45$ fm the lower range of K_0 values gets narrower, i.e., $K_0 \in [230; 250]$ MeV and, hence, $T_c \in [13.2; 14.3]$ MeV, while for the inequality $R \leqslant 0.4$ fm there are no allowed values of K_0 from the lower range of values as one can see from Fig. 3. In other words, the constraint $R \leqslant 0.4$ fm rules out the values of the incompressibility $K_0 < 250$ MeV, while it is consistent with the results of Ref. [17].
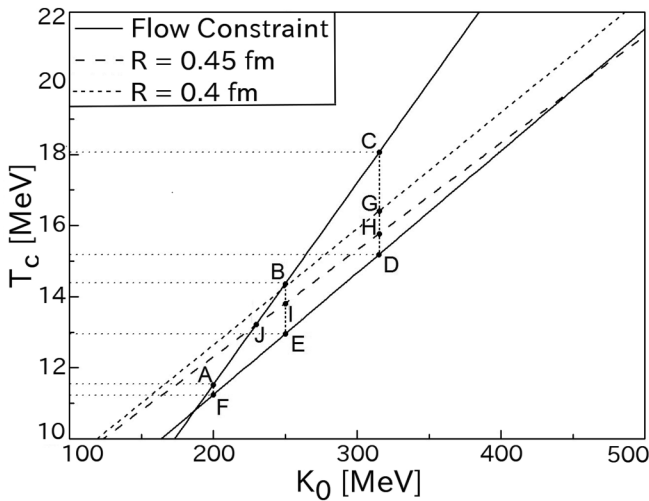

FIG. 3. Values of incompressibility constant K_0 and critical temperature T_C, which obey the proton flow constraint are located between the lines ABC and FED. The lines ABC and FED are, respectively, generated by the lower and upper branches of the proton flow constraint. The vertical lines AF, BE, and CD correspond to K_0 values 200 MeV, 250 MeV, and 315 MeV, respectively.

The determined range of K_0 and T_c values allows us to reveal the mutual consistency of experimental results. Thus, the recent experimental estimates of the nuclear matter critical temperature belong to the following range: 15.5 MeV $\lesssim T_c \lesssim$ 21 Me [2,30–32]. From Fig. 3 one can see that the values $T_c > 18$ MeV are inconsistent with the upper range of K_0 values, i.e., the critical temperature values above 18 MeV require K_0 values above 315 MeV. On the other hand the region 15.5 MeV $\lesssim T_c \lesssim$ 18 MeV is consistent with the following range of values of incompressibility constant $K_0 \in [270; 315]$ MeV. It is interesting that these ranges of T_c and K_0 values are consistent with the inequality on the nucleon hard-core radius $R \leqslant 0.35$ fm. The latter is just about 17% above the value $r \simeq 0.3$ fm used in the realistic nucleon-nucleon interaction potential to reproduce the low-energy nucleon-nucleon scattering data [33,34].

Although the values of T_c and K_0 are very well consistent with the ones found for the RMF models [12,13], the other characteristics of CEP, namely the pressure p_c, the particle number density n_c, and the compressibility constant $Z_c = \frac{p_c}{T_c n_c}$, are essentially lower than the ones found by the RMF as one can see from Table I. Surprisingly, the found $Z_c \in [0.117; 0.249]$ values demonstrate a rich diversity, but all of them are in the range of values known for real liquids, namely $Z_c \simeq 0.117$ corresponds to the hydrogen fluoride, whereas $Z_c \simeq 0.249$ corresponds to the hydrogen chloride [35]. Among other real liquids that fall into the found range of Z_c values we would mark the deuterium oxide ($Z_c \simeq 0.228$), ammonia ($Z_c \simeq 0.244$), water ($Z_c \simeq 0.229$), acetic acid ($Z_c \simeq 0.201$), acetone ($Z_c \simeq 0.232$), acetonitrile ($Z_c \simeq 0.185$), metanol ($Z_c \simeq 0.223$) [35], etc. At the same time the range of the critical compressibility constant of the RMF models is $Z_c^{\text{RMF}} \in [0.284; 0.331]$ [13], i.e., it is close or slightly above the critical compressibility constants of the following substances [35]: Ar, Kr, Xe, CH_4, N_2, O_2, and CO, but there is no reason to believe that there is a close similarity between the properties of particularly these atomic/molecular gases and the gas of nucleons. Therefore, *a priori* for the realistic EoS one would expect an essentially wider spectrum of Z_c values, like the RMF models show for T_c, n_c, and p_c values.

Of course, one may be surprised by the low values of the critical density found within the IST EoS, but we would like to remind the reader that all experimental estimates of n_c and p_c are the model-dependent ones. Furthermore, one should remember that our estimates for n_c and p_c correspond to a nuclear matter, while in the experiments one cannot ignore the Coulomb interaction. Since there is no exact way to account for the Coulomb interaction, then an extraction of the nuclear matter critical properties is inevitably a model-dependent procedure. Moreover, it is clear that, if in addition we include into a model EoS with a fixed value of κ a repulsive Coulomb-like (i.e., weak) interaction of large, but finite range, this would increase the attraction strength C_d^2 to compensate the shift of binding energy. This is apparent, since the long-range repulsion will affect the low-density characteristics, namely it will increase the pressure and binding energy per nucleon. The increase of C_d^2 will, in turn, increase the critical density and critical pressure (see the columns of same κ values in Table I). Such a modification, however, will make the whole treatment

too complicated and will destroy the main attractive feature of this model, namely its simplicity.

Besides, the typical values of n_c^{RMF} obtained in the RMF models analyzed in Ref. [13] are as follows: $n_c^{\text{RMF}} \in [0.295 \, n_0; 0.343 \, n_0]$. Suppose that these are, indeed, the true values of nuclear matter critical density. Then, if one included into these EoS a repulsive Coulomb-like interaction of large, but finite, range, it immediately would increase the critical density further, i.e., one would expect that the critical density in the real systems studied in experiments should be larger than n_c^{RMF}. In this case, however, one faces a severe problem to explain how it occurs that the experimental data on size (charge) distribution of nuclear fragments demonstrate a power law, which is typical for the CEP [2,37,38] and, moreover, how it occurs that the statistical multifragmentation model [36], which up to now is the most successful one in explaining the data obtained in the multifragmentation reactions, is able to reproduce the mentioned power law with the break-up density $n_{br} \simeq \frac{1}{6}n_0 - \frac{1}{3}n_0$ [2,36]. On the other hand, the low values of critical density obtained within the IST EoS do not face such a problem. Therefore, it seems that the typical values of n_c^{RMF} reported in Ref. [13] may evidence some internal inconsistency of these models.

IV. CONCLUSIONS

In this work we developed a novel family of EoS for symmetric nuclear matter based on the IST concept for the hard-core repulsion. It seems that the quantum version of the IST EoS employed here catches the right physics, since by having only four adjustable parameters each formulation of this EoS is able to reproduce not only the main properties of the nuclear matter ground state (three conditions), but, simultaneously, it is able to obey the proton flow constraint [14] up to particle number density 0.75 fm^{-3} (at least eight conditions). Moreover, one can easily check that all versions of the IST EoS presented here automatically obey the kaon production constraint [29].

A detailed analysis of the proton flow constraint allows us to obtain the band of values for the incompressibility constant of normal nuclear matter K_0 and the critical temperatures T_c, which are consisted with the proton flow constraint. Assuming that the quantum IST EoS is valid up to the maximal packing fraction $\eta_{\text{max}} = 0.2$ and requiring that it holds for maximal particle number density of the proton flow constraint 0.75 fm^{-3}, we obtained the condition $R \leqslant 0.4$ fm for the hard-core radius of nucleons. This condition rules out the K_0 values below 250 MeV. Furthermore, analyzing the recent data on the critical temperature value $T_c \simeq 15.5$–21 MeV, which, apparently, are not very accurate, we conclude that only the range $T_c \simeq 15.5$–18 MeV is consistent with the values $K_0 \simeq$ 270–315 MeV, while the larger values of T_c require K_0 values above 315 MeV, which are not supported by the recent findings [17]. It is interesting that the mutually consistent values of K_0 and T_c are also consistent with the inequality $R \leqslant 0.35$ fm for the hard-core radius of nucleons. This is a remarkable finding since the value 0.35 fm is just 17% above the radius of nucleon-nucleon interaction potential and at the same time this is just the hard-core radius of baryons found recently by the IST formulation of the hadron resonance gas model

from fitting the experimental hadron multiplicities measured in central nuclear collisions in the whole range of collision energies from $\sqrt{s_{NN}} = 2.7$ GeV to $\sqrt{s_{NN}} = 2.76$ TeV [23–25]. Therefore, we conclude that the physically most justified range of these quantities is as follows: $K_0 \simeq 270$–315 MeV and $T_c \simeq 15.5$–18 MeV. Based on these results, we hope that our systematic analysis of the correlations between the K_0 and T_c values will help to establish the mutual consistency of their values found with higher accuracy.

The obtained hard-core radii of nucleons are essentially smaller than the ones found recently within the novel approach of Ref. [15]. It seems that $R \geqslant 0.53$ fm claimed in [15] are highly unrealistic, since in the IST EoS they correspond to very low values of $T_c \simeq 11.16$–11.3 MeV and $K_0 \simeq 192$–199 MeV (see the column $\kappa = 0.3$ in Table I). It seems that such values are generated by the parametrization of internuclear attraction, which is typical for ordinary liquids used in Ref. [15]. This conclusion is supported by a success of the mean-field parametrization (9) employed here. We would like to point out that the interaction pressure (9), as it was first found in Ref. [18], cannot be expanded into a Taylor series at $n = 0$ and, hence, the traditional virial expansion cannot be established for this family of IST EoS. We hope that further studies of the EoS of dense quantum liquids with strong interaction will clarify the question whether the nonanalytic density dependence of pressure (9) is an inherent property of nuclear Fermi liquid or it is common for other Fermi liquids.

In contrast to the RMF models, the developed family of EoS demonstrates a wide diversity of values of the critical compressibility constant Z_c, namely $Z_c \simeq 0.117$–0.249, which, however, are well known for the ordinary liquids. Therefore, we hope it can be straightforwardly applied to the quantum and classical liquids, to which the RMF models discussed here, apparently, cannot be applied.

[1] H. Stöcker and W. Greiner, Phys. Rep. **137**, 277 (1986).

[2] V. A. Karnaukhov, Phys. Part. Nucl. **37**, 165 (2006), and references therein.

[3] J. M. Lattimer, Annu. Rev. Nucl. Part. Sci. **62**, 485 (2012), and references therein.

[4] N. Buyukcizmeci, A. S. Botvina, and I. N. Mishustin, Astrophys. J. **789**, 33 (2014).

[5] M. Dutra, O. Lourenço, S. S. Avancini, B. V. Carlson, A. Delfino, D. P. Menezes, C. Providência, S. Typel, and J. R. Stone, Phys. Rev. C **90**, 055203 (2014), and references therein.

[6] E. E. Kolomeitsev, K. A. Maslov, and D. N. Voskresensky, Nucl. Phys. A **961**, 106 (2017).

[7] K. A. Bugaev, Phys. Part. Nucl. **38**, 447 (2007).

[8] K. A. Bugaev, A. I. Ivanytskyi, V. V. Sagun, and D. R. Oliinychenko, Phys. Part. Nucl. Lett. **10**, 508 (2013).

[9] V. Sagun, A. Ivanytskyi, K. Bugaev, and I. Mishustin, Nucl. Phys. A **924**, 24 (2014).

[10] K. A. Bugaev and P. T. Reuter, Ukr. J. Phys. **52**, 489 (2007).

[11] S. Mallik, F. Gulminelli, and G. Chaudhuri, Phys. Rev. C **92**, 064605 (2015).

[12] O. Lourenço, B. M. Santos, M. Dutra, and A. Delfino, Phys. Rev. C **94**, 045207 (2016).

[13] O. Lourenço, M. Dutra, and D. P. Menezes, Phys. Rev. C **95**, 065212 (2017).

[14] P. Danielewicz, R. Lacey, and W. G. Lynch, Science **298**, 1593 (2002).

[15] V. Vovchenko, Phys. Rev. C **96**, 015206 (2017)

[16] K. A. Bugaev et al., arXiv:1704.06846 [nucl-th].

[17] J. R. Stone, N. J. Stone, and S. A. Moszkowski, Phys. Rev. C **89**, 044316 (2014).

[18] M. I. Gorenstein et al., J. Phys. G **19**, L69 (1993).

[19] M. Taketani, S. Nakamura, and M. Sasaki, Prog. Theor. Phys. **6**, 581 (1951).

[20] R. Machleidt, Adv. Nucl. Phys. **19**, 189 (1989).

[21] F. Gross, J. W. Van Orden, and K. Holinde, Phys. Rev. C **45**, 2094 (1992).

[22] D. H. Rischke, M. I. Gorenstein, H. Stöcker, and W. Greiner, Z. Phys. C **51**, 485 (1991).

[23] K. A. Bugaev et al., Nucl. Phys. A **970**, 133 (2018).

[24] V. V. Sagun et al., arXiv:1703.00049 [nucl-th].

[25] K. A. Bugaev et al., arXiv:1709.05419 [hep-ph].

[26] G. Zeeb, K. A. Bugaev, P. T. Reuter, and H. Stöcker, Ukr. J. Phys. **53**, 279 (2008).

[27] V. V. Sagun, I. Lopes, and A. I. Ivanytskyi, arXiv:1805.04976 [astro-ph.HE].

[28] T. Klähn, D. Blaschke, S. Typel, E. N. E. van Dalen, A. Faessler, C. Fuchs, T. Gaitanos, H. Grigorian, A. Ho, E. E. Kolomeitsev, M. C. Miller, G. Röpke, J. Trümper, D. N. Voskresensky, F. Weber, and H. H. Wolter, Phys. Rev. C **74**, 035802 (2006).

[29] W. G. Lynch et al., Prog. Part. Nucl. Phys. **62**, 427 (2009).

[30] V. A. Karnaukhov et al., Nucl. Phys. A **780**, 91 (2006).

[31] V. A. Karnaukhov, Phys. At. Nucl. **71**, 2067 (2008).

[32] J. B. Elliott, P. T. Lake, L. G. Moretto, and L. Phair, Phys. Rev. C **87**, 054622 (2013).

[33] See, e.g., A. Bohr and B. Mottelson, *Nuclear Structure* (Benjamin, New York 1969), Vol. 1.

[34] A. Andronic, P. Braun-Munzinger, and J. Stachel, Nucl. Phys. A **772**, 167 (2006), and references therein.

[35] Kaye and Laby, *Tables of Physical and Chemical Constants*, Sec. 3.5, National Physical Laboratory, UK, http://www.kayelaby. npl.co.uk/chemistry/3_5/3_5.html

[36] J. P. Bondorf *et al.*, Phys. Rep. **257**, 133 (1995), and references therein.

[37] J. B. Elliott, S. Albergo, F. Bieser, F. P. Brady, Z. Caccia, D. A. Cebra, A. D. Chacon, J. L. Chance, Y. Choi, S. Costa, M. L. Gilkes, J. A. Hauger, A. S. Hirsch, E. L. Hjort, A. Insolia, M. Justice, D. Keane, J. C. Kintner, V. Lindenstruth, M. A. Lisa, H. S. Matis, M. McMahan, C. McParland, W. F. J. Muller, D. L. Olson, M. D. Partlan, N. T. Porile, R. Potenza, G. Rai, J. Rasmussen, H. G. Ritter, J. Romanski, J. L. Romero, G. V. Russo, H. Sann, R. P. Scharenberg, A. Scott, Y. Shao, B. K. Srivastava, T. J. M. Symons, M. Tincknell, C. Tuve, S. Wang, P. G. Warren, H. H. Wieman, T. Wienold, and K. Wolf (EOS Collaboration), Phys. Rev. C **62**, 064603 (2000).

[38] P. T. Reuter and K. A. Bugaev, Phys. Lett. B **517**, 233 (2001).